

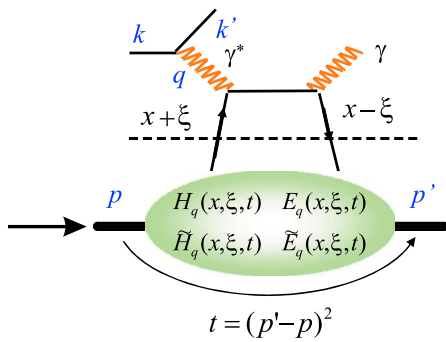
Precision DVCS cross sections and extraction of CFFs

Carlos Muñoz Camacho

Laboratoire Irène Joliot-Curie, CNRS/IN2P3 (France)

REVESTSTRUCTURE workshop
Zagreb, July 10–12 2023

Deeply Virtual Compton Scattering (DVCS): $\gamma^* p \rightarrow \gamma p$



High Q^2
Perturbative QCD

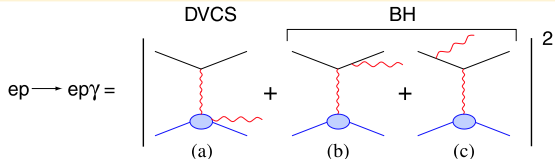
Non-perturbative GPDs

Handbag diagram

Bjorken limit :

$$Q^2 = \begin{array}{c} -q^2 \\ \nu \end{array} \rightarrow \begin{array}{c} \infty \\ \infty \end{array} \left. \right\} x_B = \frac{Q^2}{2M\nu} \text{ fixed}$$

DVCS experimentally: interference with Bethe-Heitler



At leading order in $1/Q$ (leading twist) :

$$d^5 \vec{\sigma} - d^5 \overleftarrow{\sigma} = \mathfrak{Im}(T^{BH} \cdot T^{DVCS})$$

$$d^5 \vec{\sigma} + d^5 \overleftarrow{\sigma} = |BH|^2 + \textcolor{teal}{Re}(T^{BH} \cdot T^{DVCS}) + |DVCS|^2$$

$$\mathcal{T}^{DVCS} = \int_{-1}^{+1} dx \frac{H(x, \xi, t)}{x - \xi + i\epsilon} + \dots =$$

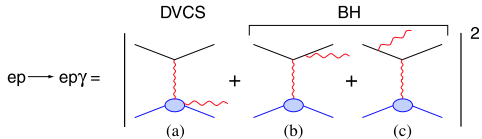
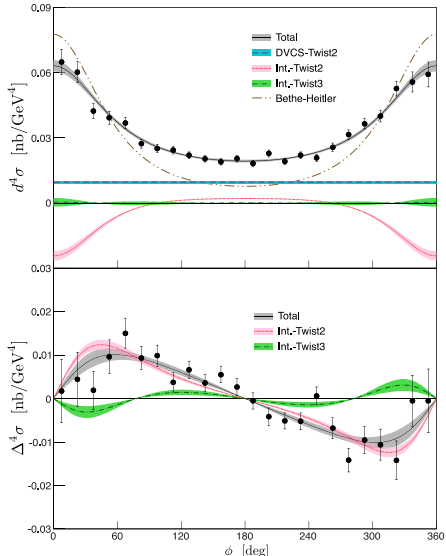
$$\underbrace{\mathcal{P} \int_{-1}^{+1} dx \frac{H(x, \xi, t)}{x - \xi}}_{-} - \underbrace{i\pi H(x = \xi, \xi, t)}_{+} + \dots$$

Access in helicity-independent cross section

Access in helicity-dependent cross-section

DVCS cross sections: azimuthal analysis

$$Q^2 = 2.36 \text{ GeV}^2, x_B = 0.37, -t = 0.32 \text{ GeV}^2$$



$$d^4\sigma = \mathcal{T}_{\text{BH}}^2 + \mathcal{T}_{\text{BH}} \text{Re}(\mathcal{T}_{\text{DVCS}}) + \mathcal{T}_{\text{DVCS}}^2$$

$$\text{Re}(\mathcal{T}_{\text{DVCS}}) \sim c_0^{\mathcal{I}} + c_1^{\mathcal{I}} \cos \phi + c_2^{\mathcal{I}} \cos 2\phi$$

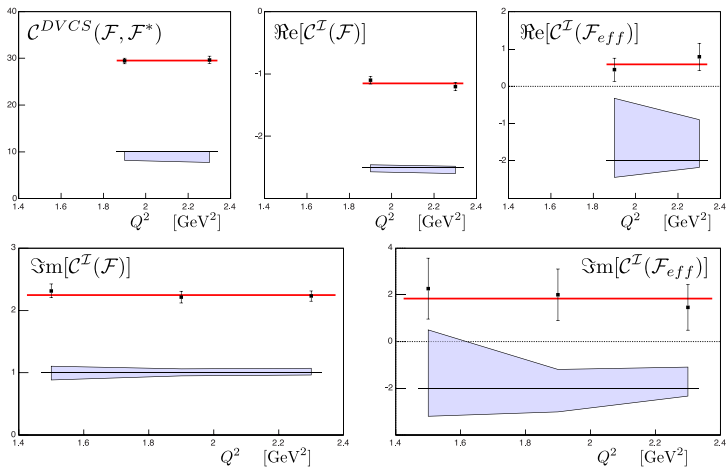
$$\mathcal{T}_{\text{DVCS}}^2 \sim c_0^{\text{DVCS}} + c_1^{\text{DVCS}} \cos \phi$$

$$\Delta^4\sigma = \frac{d^4\vec{\sigma} - d^4\overleftarrow{\sigma}}{2} = \text{Im}(\mathcal{T}_{\text{DVCS}})$$

$$\text{Im}(\mathcal{T}_{\text{DVCS}}) \sim s_1^{\mathcal{I}} \sin \phi + s_2^{\mathcal{I}} \sin 2\phi$$

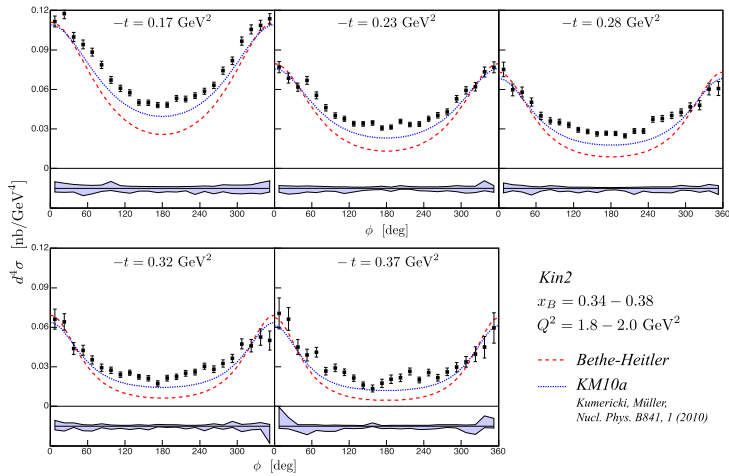
M. Defurne et al. Phys. Rev. C92, 055202 (2015)

DVCS cross sections: Q^2 -dependance



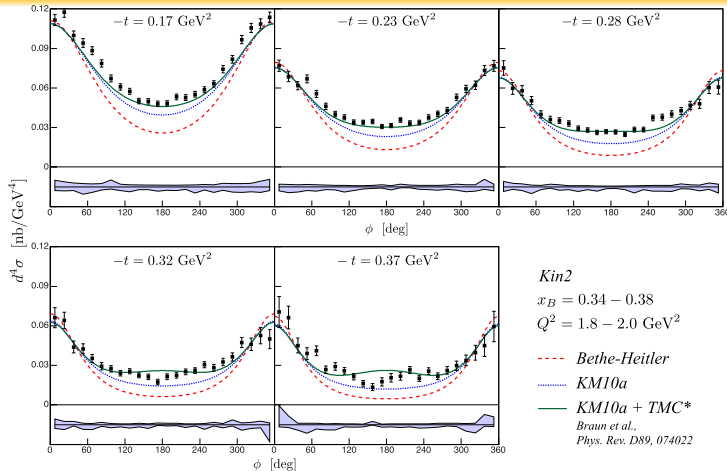
No Q^2 -dependance within limited range \Rightarrow leading twist dominance

DVCS cross sections: kinematical power corrections



- KM10a: global fit to HERA x-sec & HERMES + CLAS spin asymmetries
Kumericki and Mueller (2010)

DVCS cross sections: kinematical power corrections



- KM10a: global fit to HERA x-sec & HERMES + CLAS spin asymmetries
Kumericki and Mueller (2010)
- Target-mass corrections (TMC): $\sim \mathcal{O}(M^2/Q^2)$ and $\sim \mathcal{O}(t/Q^2)$
Braun, Manashov, Mueller and Pirnay (2014)

Rosenbluth-like separation of the DVCS cross section

$$\sigma(ep \rightarrow ep\gamma) = \underbrace{|BH|^2}_{\text{Known to } \sim 1\%} + \underbrace{\mathcal{I}(BH \cdot DVCS)}_{\text{Linear combination of GPDs}} + \underbrace{|DVCS|^2}_{\text{Bilinear combination of GPDs}}$$

$\mathcal{I} \propto 1/y^3 = (k/\nu)^3,$

$|\mathcal{T}^{DVCS}|^2 \propto 1/y^2 = (k/\nu)^2$

BKM-2010 – at leading twist \rightarrow 7 independent GPD terms:

$$\{\Re, \Im [C^I, C^{I,V}, C^{I,A}] (\mathcal{F})\}, \quad \text{and} \quad C^{DVCS}(\mathcal{F}, \mathcal{F}^*).$$

φ -dependence provides 5 independent observables:

$$\sim 1, \sim \cos \varphi, \sim \sin \varphi, \sim \cos(2\varphi), \sim \sin(2\varphi)$$

The measurement of the cross section at **two or more beam energies** for exactly the **same Q^2 , x_B , t kinematics**, provides the additional information in order to extract all leading twist observables independently.

DVCS process: leading twist ambiguity

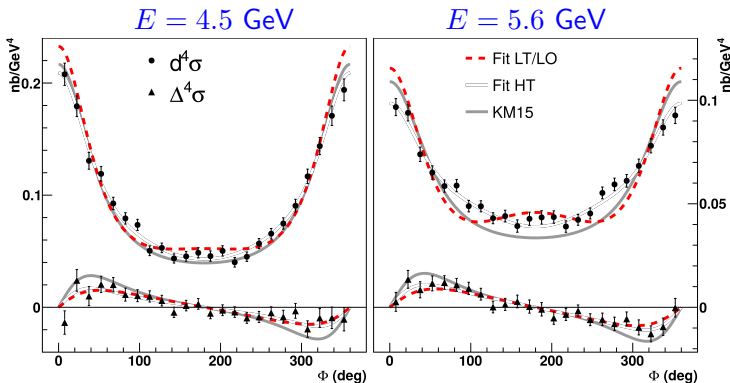
- DVCS defines a preferred axis: light-cone axis
- At finite Q^2 and non-zero t , there is an ambiguity:
 - ➊ Belitsky et al. ("BKM", 2002–2010): light-cone axis in plane (q, P)
 - ➋ Braun et al. ("BMP", 2014): light-cone axis in plane (q, q')
easier to account for kin. corrections $\sim \mathcal{O}(M^2/Q^2)$, $\sim \mathcal{O}(t/Q^2)$

$$\left. \begin{array}{l} \mathcal{F}_{++} = \mathbb{F}_{++} + \frac{\chi}{2} [\mathbb{F}_{++} + \mathbb{F}_{-+}] - \chi_0 \mathbb{F}_{0+} \\ \mathcal{F}_{-+} = \mathbb{F}_{-+} + \frac{\chi}{2} [\mathbb{F}_{++} + \mathbb{F}_{-+}] - \chi_0 \mathbb{F}_{0+} \\ \mathcal{F}_{0+} = -(1 + \chi) \mathbb{F}_{0+} + \chi_0 [\mathbb{F}_{++} + \mathbb{F}_{-+}] \end{array} \right\} \xrightarrow{\begin{array}{l} \mathbb{F}_{-+} = 0 \\ \mathbb{F}_{0+} = 0 \end{array}} \left\{ \begin{array}{l} \mathcal{F}_{++} = (1 + \frac{\chi}{2}) \mathbb{F}_{++} \\ \mathcal{F}_{-+} = \frac{\chi}{2} \mathbb{F}_{++} \\ \mathcal{F}_{0+} = \chi_0 \mathbb{F}_{++} \end{array} \right.$$

(eg. $\chi_0 = 0.25$, $\chi = 0.06$ for $Q^2 = 2$ GeV 2 , $x_B = 0.36$, $t = -0.24$ GeV 2)

E07-007: DVCS beam-energy dependence

- Cross section measured at 2 beam energies and constant Q^2 , x_B , t



- Leading-twist and LO simultaneous fit of both beam energies (dashed line) does not reproduce the data

Light-cone axis in the (q, q') plane (Braun et al.): \mathbb{H}_{++} , $\widetilde{\mathbb{H}}_{++}$, \mathbb{E}_{++} , $\widetilde{\mathbb{E}}_{++}$

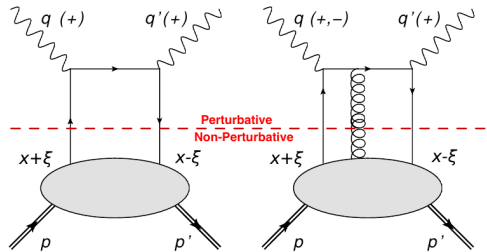
Beyond Leading Order (LO) and Leading Twist (LT)

Two fit-scenarios:

Light-cone axis in
the (q, q') plane (Braun et al.)

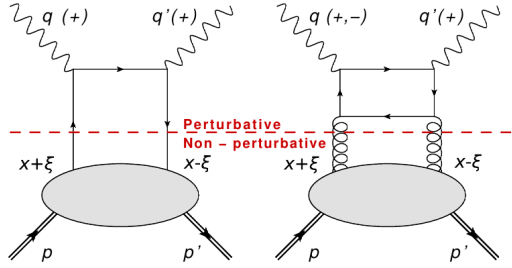
LO/LT + HT

$\mathbb{H}_{++}, \tilde{\mathbb{H}}_{++}, \mathbb{H}_{0+}, \tilde{\mathbb{H}}_{0+}$



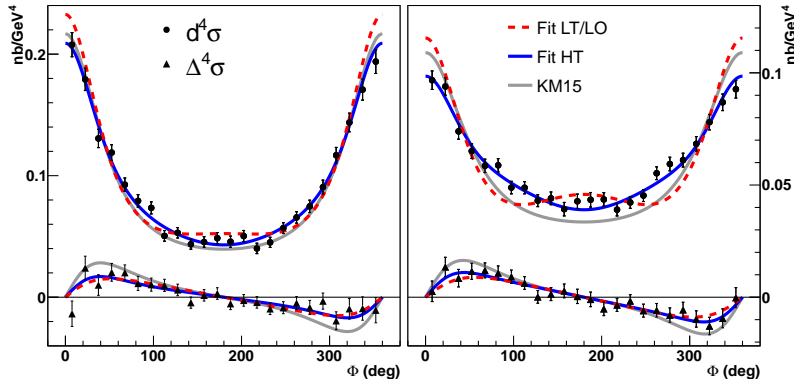
LO/LT + NLO

$\mathbb{H}_{++}, \tilde{\mathbb{H}}_{++}, \mathbb{H}_{-+}, \tilde{\mathbb{H}}_{-+}$



E07-007: DVCS beam-energy dependence

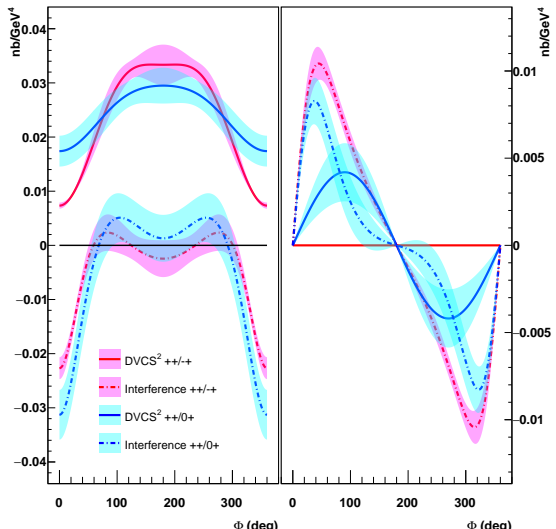
- Cross section measured at 2 beam energies and constant Q^2 , x_B , t



- Leading-twist and LO simultaneous fit of both beam energies (dashed line) does not reproduce the data
- Including either NLO or higher-twist effects (dark solid line) satisfactorily reproduce the angular dependence

DVCS² and \mathcal{I} (DVCS·BH) separation

DVCS² and \mathcal{I} (DVCS·BH) separated in NLO and higher-twist scenarios



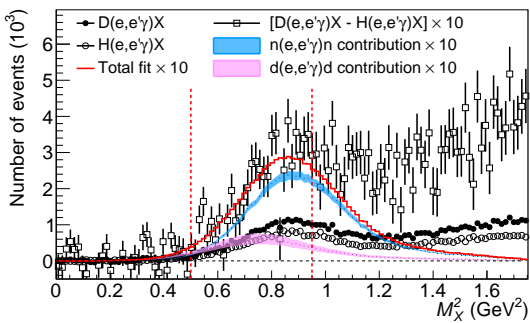
- DVCS² & \mathcal{I} significantly different in each scenario
- Sizeable DVCS² contribution in the higher-twist scenario in the helicity-dependent cross section

Nature Commun. 8, 1408 (2017)

E08-025: DVCS off the neutron at different beam energies

- LD₂ as a target ($Q^2 = 1.75 \text{ GeV}^2, x_B = 0.36$)
- Quasi-free p evts subtracted using the (normalized) data from E07-007
- Concurrent running: switching LD2/LD2 → minimize uncertainties

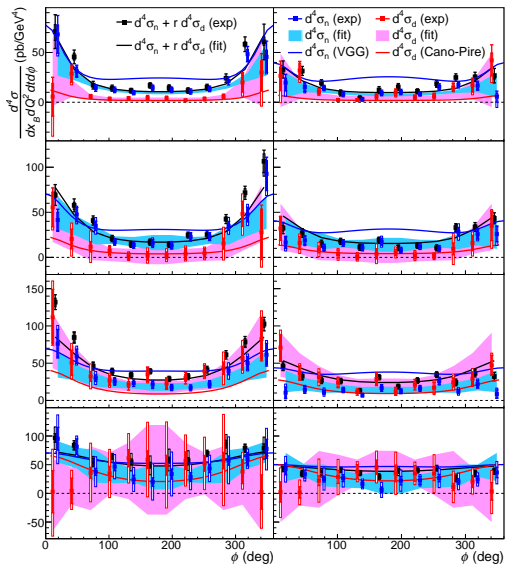
$$D(e, e\gamma)X - p(e, e\gamma)p = n(e, e\gamma)n + d(e, e\gamma)d$$



nDVCS & dDVCS
shifted by $t/2$ in M_X^2

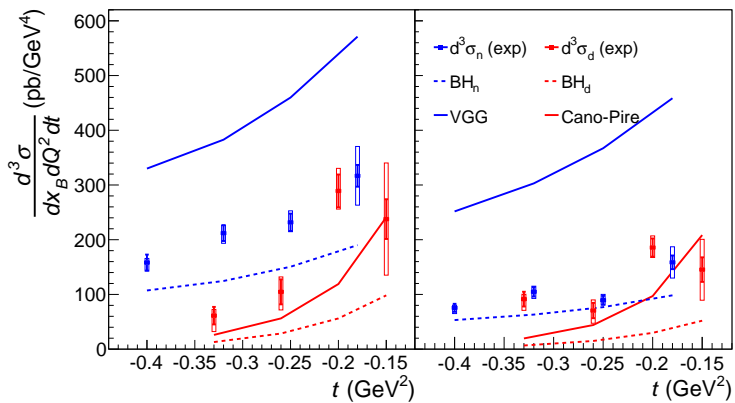
DVCS cross sections off the n & d

- Large correlations at low $-t$
- Good separation at larger $-t$
- dDVCS very small
(compatible with theory)
- nDVCS: significant signal
(first observation of DVCS off the nucleon)



M. Benali et al., Nature Physics 16, 191 (2020)

DVCS off the neutron: t -dependence



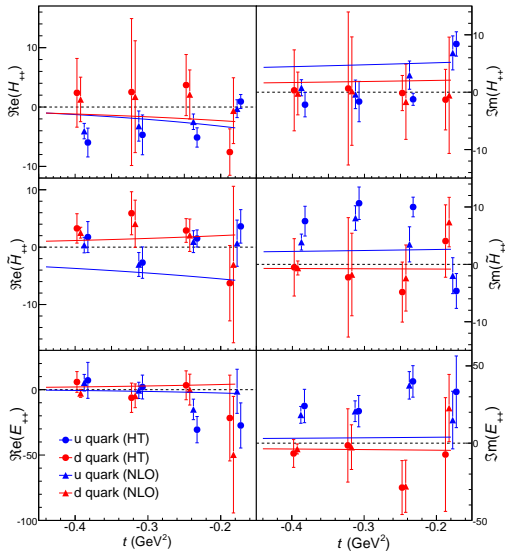
- First experimental determination of the unpolarized $en \rightarrow e\gamma n$ cross section
- $\sigma(en \rightarrow e\gamma n) > \sigma(BH_n)$: **Sizeable DVCS off the neutron**

M. Benali et al., Nature Physics 16, 191 (2020)

DVCS off the neutron: flavor-separated CFFs

Global fit of all Hall A DVCS data off proton & neutron, with CFFs of up and down quarks as free parameters

- H^u and H^d : same sign (as forward & large N_c limits, models...)
- \tilde{H}^u and \tilde{H}^d : opposite sign (as forward & large N_c limit, models...)
- Data suggest same sign for $\text{Re}(E^u)$ and $\text{Re}(E^d)$ (against predictions from the large N_c limit)

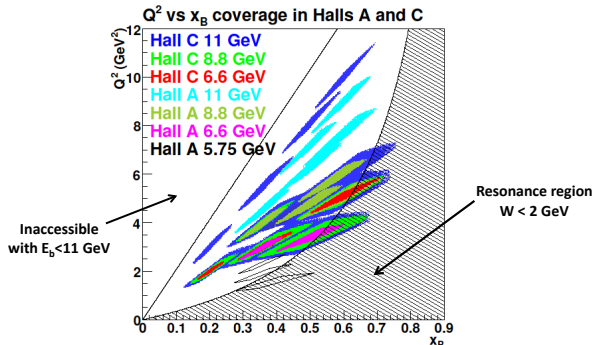


M. Benali et al., Nature Physics 16, 191 (2020)

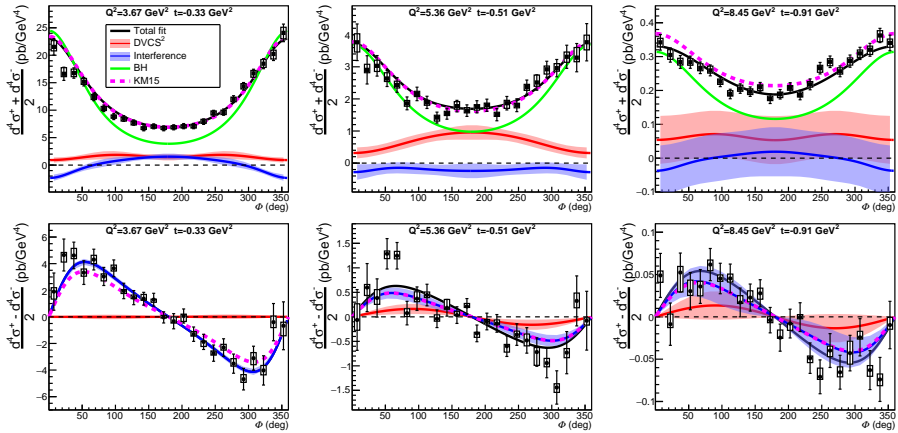
E12-06-114: DVCS at 12 GeV

Setting	Kin-36-1	Kin-36-2	Kin-36-3	Kin-48-1	Kin-48-2	Kin-48-3	Kin-48-4	Kin-60-1	Kin-60-3
x_B	0.36				0.48				0.60
E_b (GeV)	7.38	8.52	10.59	4.49	8.85	8.85	10.99	8.52	10.59
Q^2 (GeV 2)	3.20	3.60	4.47	2.70	4.37	5.33	6.90	5.54	8.40
E_γ (GeV)	4.7	5.2	6.5	2.8	4.7	5.7	7.5	4.6	7.1
$-t_{min}$ (GeV 2)	0.16	0.17	0.17	0.32	0.34	0.35	0.36	0.66	0.70
$\int Q dt$ (C)	1.2	1.7	1.3	2.2	2.2	3.7	5.7	6.4	18.5
# data bins	672			912				480	

E12-06-114 kinematics



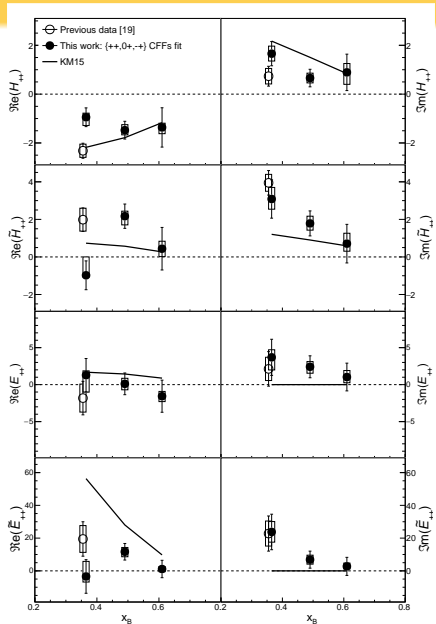
E12-06-114: DVCS at 12 GeV



F. Georges et al., Phys. Rev. Lett. 128 (2022)

E12-06-114: CFFs extraction

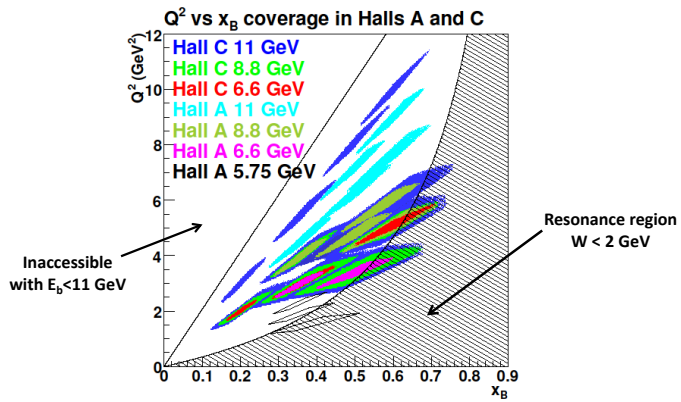
- Extraction of all CFFs ($++, 0+, -+$) as a function of x_B
- GPD H well constraint
- Sensitivity to E and \tilde{E}



F. Georges et al., Phys. Rev. Lett. 128 (2022)

Upcoming DVCS run in Hall C (2023–2024)

- Energy dependence at most of the $Q^2 - x_B$ settings
- Additional Q^2 points
- Additional settings at low x_B



Summary

- Recent high precision DVCS cross sections from Hall A at JLab
- Need of higher twist and/or NLO contributions to fully describe the data (eg. in global GPD fits)
- First separation of DVCS² and BH-DVCS interference in the $eN \rightarrow e\gamma N$ cross section, off the proton and neutron
- Approved program of experiments in Hall A and C to continue these high precision DVCS measurements at 12 GeV

Back-up

π^0 electroproduction ($ep \rightarrow ep\pi^0$)

At leading twist:

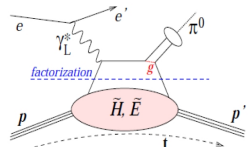
$$\frac{d\sigma_L}{dt} = \frac{1}{2}\Gamma \sum_{h_N, h_{N'}} |\mathcal{M}^L(\lambda_M = 0, h'_N, h_N)|^2 \propto \frac{1}{Q^6} \quad \sigma_T \propto \frac{1}{Q^8}$$

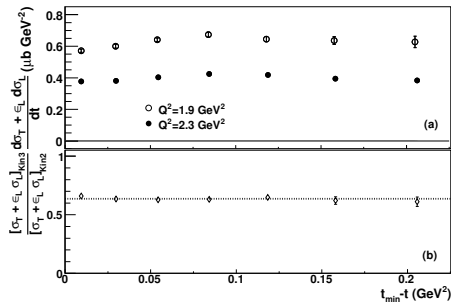
$$\mathcal{M}^L \propto \left[\int_0^1 dz \frac{\phi_\pi(z)}{z} \right] \int_{-1}^1 dx \left[\frac{1}{x - \xi} + \frac{1}{x + \xi} \right] \times \left\{ \Gamma_1 \tilde{H}_{\pi^0} + \Gamma_2 \tilde{E}_{\pi^0} \right\}$$

Different quark weights: flavor separation of GPDs

$$|\pi^0\rangle = \frac{1}{\sqrt{2}}\{|u\bar{u}\rangle - |d\bar{d}\rangle\} \quad \tilde{H}_{\pi^0} = \frac{1}{\sqrt{2}} \left\{ \frac{2}{3}\tilde{H}^u + \frac{1}{3}\tilde{H}^d \right\}$$

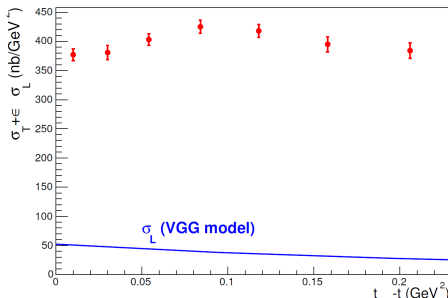
$$|p\rangle = |uud\rangle \quad H_{DVCS} = \frac{4}{9}H^u + \frac{1}{9}H^d$$



Exclusive π^0 electroproduction cross-sections

(a)

(b)



- $\sigma_T + \epsilon_L \sigma_L \sim Q^{-5}$
(similar to $\sigma_T(ep \rightarrow ep\pi^+)$ measured in Hall C)
- GPDs predict $\sigma_L \sim Q^{-6}$
- σ_T likely to dominate at these Q^2 ,
but L/T separation necessary (\rightarrow new experiment...)

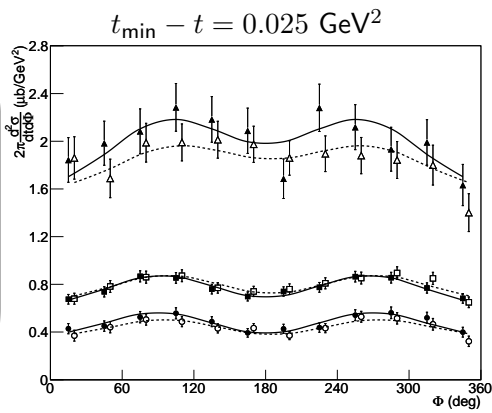
E. Fuchey et al., Phys. Rev. C83 (2011), 025125

Rosenbluth separation

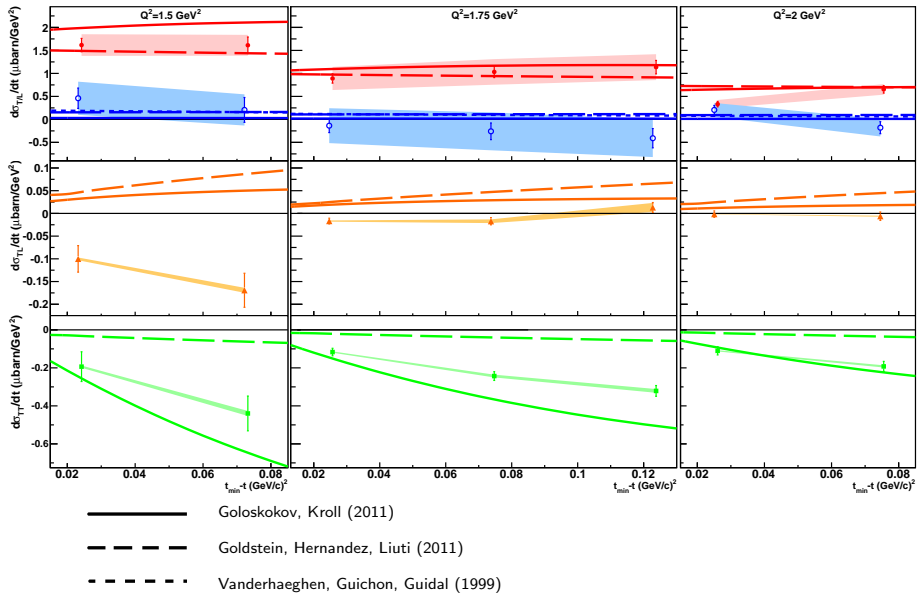
$$\frac{d^4\sigma}{dQ^2 dx_B dt d\phi} = \frac{1}{2\pi} \Gamma(Q^2, x_B, E) \left[\frac{d\sigma_T}{dt} + \epsilon \frac{d\sigma_L}{dt} + \sqrt{2\epsilon(1+\epsilon)} \frac{d\sigma_{TL}}{dt} \cos\phi + \epsilon \frac{d\sigma_{TT}}{dt} \cos^2\phi \right]$$

Kinematics

Setting	Q^2 (GeV 2)	x_B	E^{beam} (GeV)	ϵ
Kin1	1.50	0.36	3.355	0.52
			5.55	0.84
Kin2	1.75	0.36	4.455	0.65
			5.55	0.79
Kin3	2.00	0.36	4.455	0.53
			5.55	0.72



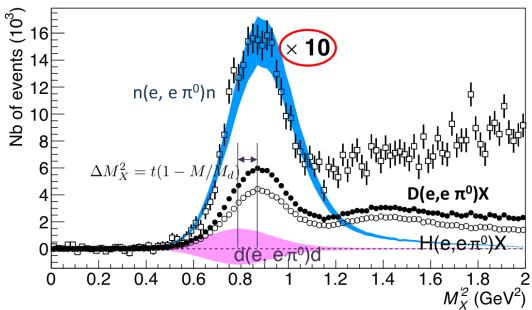
π^0 separated response functions



E08-025: DVCS and π^0 off quasi-free neutrons

- LD₂ as a target
- Quasi-free p evts subtracted using the (normalized) data from E07-007
- Concurrent running: switching LD2/LD2 → minimize uncertainties

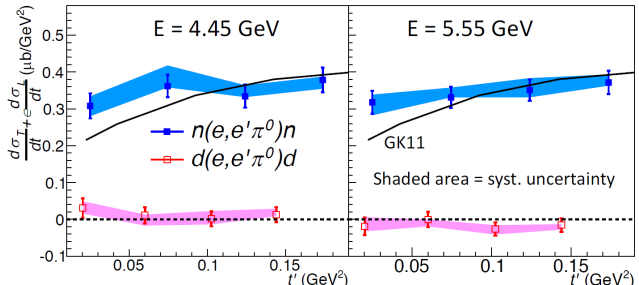
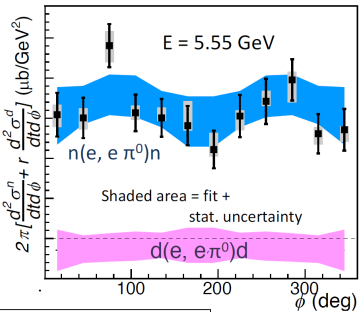
$$D(e, e \pi^0)X - p(e, e \pi^0)p = n(e, e \pi^0)n + d(e, e \pi^0)d$$



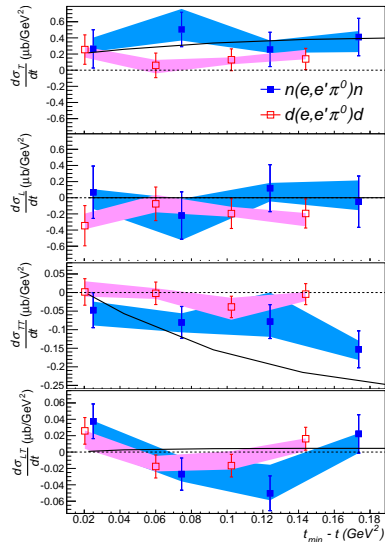
The average momentum transfer to the target is much larger than the np relative momentum, justifying this **impulse approximation**

π^0 electroproduction cross section off the neutron

- Cross section off coherent d found negligible within uncertainties
- Very low E_{beam} dependence of the n cross section → dominance of σ_T

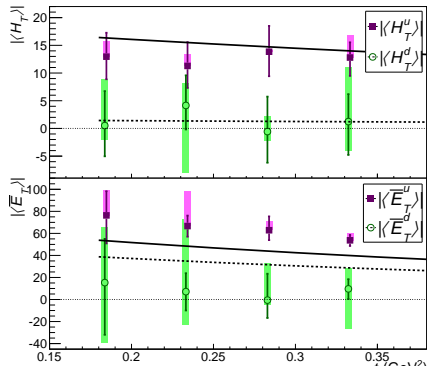


Separated π^0 cross section off the neutron



In the modified factorization approach (KG):

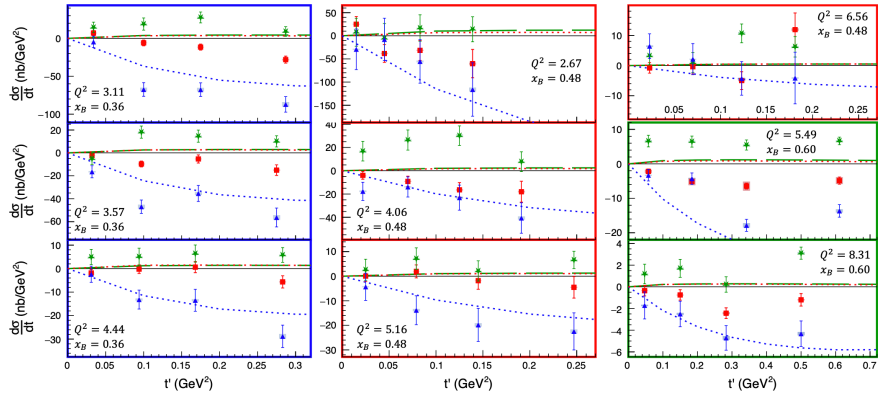
- $d\sigma_T \propto \left[(1 - \xi^2) |\langle H_T \rangle|^2 - \frac{t'}{8M^2} |\langle \bar{E}_T \rangle|^2 \right]$
- $d\sigma_{TT} \propto \frac{t'}{8M^2} |\langle \bar{E}_T \rangle|^2$



$$|\langle H_T^{p,n} \rangle|^2 = \frac{1}{2} \left| \frac{2}{3} \left\langle H_T^{u,d} \right\rangle + \frac{1}{3} \left\langle H_T^{d,u} \right\rangle \right|^2$$

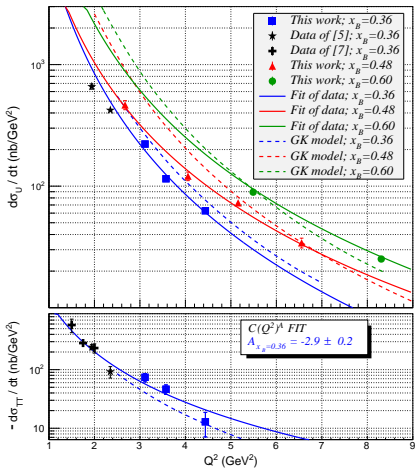
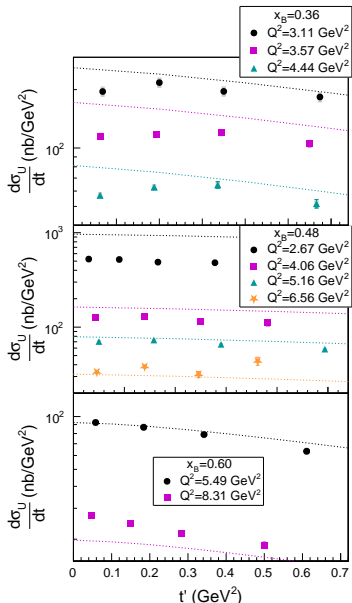
M. Mazouz et al, Phys.Rev.Lett. 118 (2017)

π^0 electroproduction at 12 GeV



- $\sigma_{TT} \gg \sigma_{TL,LT}$
- Values well described by modified factorization approach

ArXiv:2011.11125

π^0 electroproduction at 12 GeV

ArXiv:2011.11125